Available online at www.sciencedirect.com
ScienceDirect
Catalysis Today 129 (2007) 240–246
CATALYSIS TODAY
www.elsevier.com/locate/cattod

Magnetic resonance study of the defects influence on the surface characteristics of nanosize anatase

J. Soria [a,*], J. Sanz [b], I. Sobrados [b], J.M. Coronado [c], F. Fresno [a], M.D. Hernández-Alonso [a]

[a] *Inst. de Catálisis y Petroleoquímica, CSIC, Cantoblanco, 28049 Madrid, Spain*
[b] *Inst. de Ciencia de Materiales, CSIC, Cantoblanco, 28049 Madrid, Spain*
[c] *Aplicaciones Medioambientales de la Energía Solar, CIEMAT, Av. Complutense 22, 28040 Madrid, Spain*

Abstract

Two anatase samples with crystal size of 11 and 6 nm, prepared by thermal, P11T, and hydrothermal treatments, P6H, of an amorphous TiO_2 precursor, have been studied by ^1H nuclear magnetic resonance (NMR) and electron paramagnetic resonance (EPR) to obtain information on how the samples defects influence their surface characteristics. The NMR spectra of the hydrated samples were mainly originated by weakly adsorbed water, more abundant on P6H than on P11T, while most of the spectra obtained after evacuation at 473 K were originated by hydroxyls. P6H presented a larger amount of hydroxyls, some of them with significantly different chemical shifts, than P11T. Those particular hydroxyls are generated by water dissociation at oxygen vacancies. The type and intensity of the signals observed in the EPR spectra of the UV irradiated samples depended on the samples preparation method and on the amount of water weakly adsorbed on the samples. For hydrated P6H, photogenerated electrons are stabilized by Ti^{4+} cations at oxygen vacancies, while these electrons can be delocalized in the P11T conduction band. The stabilization of photogenerated holes as O^- radicals by low coordinate bridging O^{2-}, more marked for P6H than for P11T, is favored by weakly adsorbed water. This effect has been attributed to the photodesorption of adsorbed water and protons from acidic bridging hydroxyls, as H_3O^+ species exchanging protons with adsorbed water, while the hydroxyls bridging O^{2-} anions trap photogenerated holes.

Keywords: TiO_2; Nuclear magnetic resonance; Nanoparticles; Electron paramagnetic resonance

1. Introduction

The light-induced production of charge carriers is the basic requirement for the application of semiconductors in photocatalysis [1,2]. Once produced, the charge carriers can become trapped or recombine, but can also react with electron donors or acceptors adsorbed on the photocatalyst surface [3]. Recombination and trapping of the charge carriers and the competition with interfacial charge transfer determine the overall quantum efficiency [1–3]. For photocatalytic systems in which the rate limiting step is interfacial charge transfer, improved charge separation and inhibition of charge recombination are essential for enhancing the quantum efficiency of the process [1,4]. Therefore, methods for improving photocatalytic properties, by enhancing the photocatalyst charge separation capability and/or improving interfacial charge transfer, should be addressed.

TiO_2 is the most widely used photocatalyst, because it provides the best compromise between photocatalytic performance and stability in most chemical environments [5]. In addition, it is inexpensive and essentially non-toxic, although precautions must be taken when prepared as nanoparticles [6]. Growing evidence suggests that the TiO_2 polymorph anatase, thermodynamically less stable than rutile, is more active for oxidative detoxification reactions [5]. However, the anatase photocatalytic properties need to be improved to enhance its capability for photocatalytic oxidation (PCO) of some organic pollutants [7,8]. An attractive method to modify anatase properties without introducing any new component is the preparation of TiO_2 nanoparticles, where anatase is the most probable phase when the TiO_2 grain size is around 10 nm [8]. The physical and chemical properties of TiO_2 depend largely on the surface for particles a few nanometres in size. This is particularly true for charge carriers trapping, because many

* Corresponding author. Tel.: +34 91 585 4767; fax: +34 91 585 4760.
E-mail address: jsoria@icp.csic.es (J. Soria).

0920-5861/$ – see front matter © 2007 Elsevier B.V. All rights reserved.
doi:10.1016/j.cattod.2007.08.001

surface defects act as trapping sites [9,10]. However, on polycrystalline surfaces, their exact nature and function are not well established.

Recent reports have shown that anatase with crystal size in the 3–11 nm range, prepared by hydrothermally treating (HT) an amorphous precursor, was a more efficient photocatalyst for toluene PCO than calcined (TT) TiO_2 with anatase crystal size in the 11–20 nm range [11]. The value of the toluene PCO steady state rate and the selectivity to CO_2 increased with decreasing crystal size down to 6 nm, for HT samples; meanwhile, for TT samples, the selectivity to CO_2 increased with decreasing crystal size, but the steady state toluene PCO rate remained practically constant. The continuous increase of the selectivity to CO_2, a photocatalyst surface property strongly dependent on the adsorbed water, with decreasing anatase crystal size indicated that some adsorbed water was being modified by decreasing the crystal size. On the other hand, the different behavior of the steady state toluene PCO rate for TT and HT samples indicated that this property was related to the anatase preparation method [12].

To get insight into the characteristics of the adsorbed water affected by variations of the anatase crystal size, in the present work we have studied, by ^{1}H NMR, the water and hydroxyls present in TT and HT samples. In addition, we have investigated, by EPR, the stabilization of photogenerated charge carriers in defects of the hydrated and evacuated samples, in order to obtain information on these defects and on their interaction with the surface hydroxyls and water.

2. Experimental

2.1. Materials

Titanium isopropoxide (TIP) was used as a precursor for the sol–gel synthesis of nanocrystalline TiO_2 catalysts. The synthesis was conducted by controlled addition of 1 ml of TIP into a well-mixed isopropanol–water solution under N_2 atmosphere [13]. The mixture was then aged for 1 h at RT and the obtained solid was recovered by filtration and dried at 338 K for 24 h. A subsequent hydrothermal treatment of the amorphous material in a water–isopropanol mixture (2/3, v/v) was carried out in a 150 ml Teflon-line autoclave vessel heated at 423 K for 8 h, which produced a crystalline sample labeled P6H. Another aliquot was calcined in air at 723 K for 3 h (sample P11T).

The TiO_2 powders were analyzed by XRD using a Philips PW 1030 X-ray diffractometer equipped with a Cu Kα radiation source and a graphite monochromator. The BET surface areas were obtained from the N_2 adsorption isotherm measured with a Micromeritics ASAP 2010 equipment.

2.2. ^{1}H NMR studies

NMR spectra were recorded in an AVANCE 400 (Bruker) spectrometer. ^{1}H NMR spectra were recorded after the irradiation of the sample with a π/2 radiofrequency pulse (single pulse technique). The ^{1}H NMR frequency used was 400.13 MHz (B_0 = 9.4 T). In MAS-NMR experiments, samples were spun at 4 and 10 kHz around an axis inclined 54°44′ with respect to the magnetic field (Magic angle spinning technique). The number of scans, 100, was selected to obtain a signal to noise ratio of 40. In order to avoid saturation effects, the chosen time between consecutive experiments was 5 s. Spectral deconvolution was carried out with the Winfit (Bruker) software package. Intensity, position and linewidth of components were determined with a non-linear least-square iterative program. Intensities were referred to that of the cap of the rotor used for MAS experiments. Chemical shift values of ^{1}H NMR components were referred to that of the TMS signal.

2.3. EPR measurements

EPR measurements were carried out with a Bruker ER200D instrument operating in the X-band. Aliquots of the catalyst were placed into a special cell made of spectroscopically pure quartz and provided with greaseless taps for evacuation and gas incorporation treatments. All the spectra were recorded at 77 K, after evacuation, in a double T-type cavity. The frequency of the microwave was calibrated for each experiment using a standard of DPPH (g = 2.0036) located in the second cavity. Computer simulations were used when necessary to check spectral parameters. Previous adsorption and/or desorption treatments of the samples were carried out in a conventional vacuum line, achieving pressures down to 10^{-4} N m^{-2}. Irradiation treatments under static conditions were carried out at 77 K by placing the cell in a quartz Dewar flask without any metallic coating. For these experiments the UV sources were four fluorescent lamps (Sylvania F6WBLB-T5 maximum intensity at 356 nm).

3. Results and discussion

The ^{1}H NMR and EPR spectra obtained for samples prepared by the same method and pretreated under slightly different conditions were relatively similar; however, the spectra of samples prepared by different methods showed clear differences. In this section, the results corresponding to P11T and P6H, representative of the thermally and hydrothermally prepared samples, respectively, will be presented.

The XRD patterns of P11T and P6H show that the only crystalline compound present in both samples is anatase. The crystal sizes calculated from the width of the (1 0 1) diffraction peak, by means of the Scherrer equation, and confirmed by transmission electron microscopy are 11 and 6 nm for P11T and P6H, respectively. The BET specific surface areas of these samples are 85 and 175 m^2/g for P11T and P6H, respectively.

3.1. ^{1}H MAS-NMR study

The ^{1}H MAS-NMR spectra of the hydrated anatase samples were mainly formed by a narrow component A at 4.0 and 5.5 ppm for P11T and P6H, respectively, Fig. 1a and b. Two small components denoted B and C hereafter were also observed at about 1.7 and 9.9 ppm, respectively, in the P6H

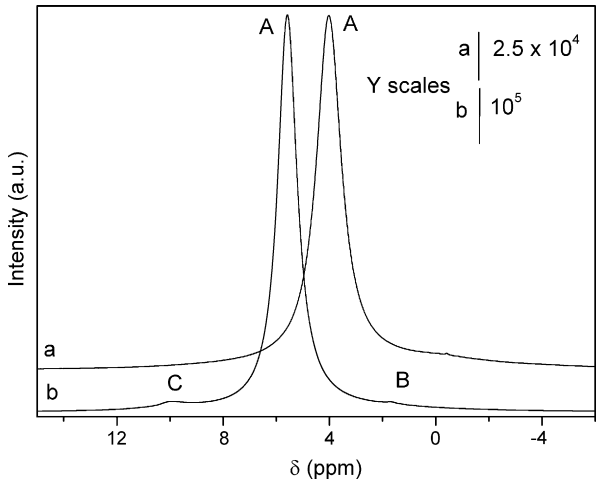

Fig. 1. ^{1}H MAS-NMR spectra of hydrated anatase: (a) P11T and (b) P6H.

spectrum. The small linewidth of the component A, which was broadened by evacuation at room temperature, indicates that it is originated by protons of very mobile water [14].

The decrease of the component A in the spectra of the samples evacuated at 473 K, Fig. 2, and the sample spinning at 10 kHz improved, considerably, the experimental resolution, favoring the detection of new components. Thus, two narrow bands, at 3.7 and 5.1 ppm, appear in the P11T spectrum, Fig. 2a; while the P6H spectrum shows two bands at 3.8 and 8.3 ppm with shoulders at 4.9 and 9.3 ppm, Fig. 2b. Both spectra also show a complex component B with its maximum, at about 0 ppm, contributing more strongly to the P6H spectra than to that of P11T, presenting a quite different shape. The bottom part of this component is formed by a broad signal with similar linewidth in both spectra. However, while the top part of the P11T spectrum is formed by several very narrow lines overlapped by the broad component, the top part of the P6H spectrum presents a relatively narrow signal, at −0.1 ppm, overlapping the broad and the very narrow signals. The broad band and the very narrow signals contributing to the complex component of both samples spectra can be associated with the

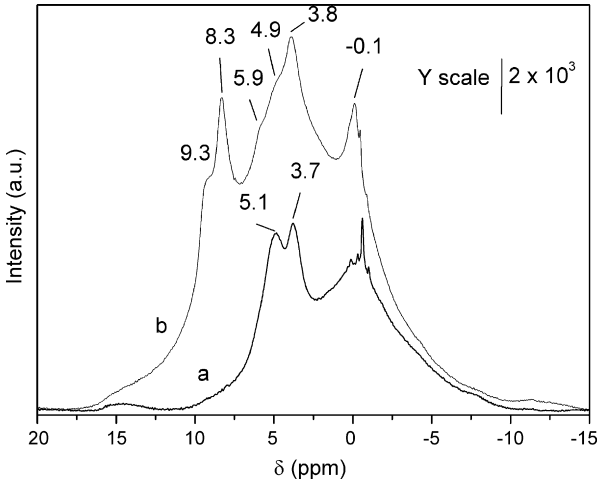

Fig. 2. ^{1}H MAS-NMR spectra of anatase evacuated at 473 K: (a) P11T and (b) P6H.

proton signal of the rotor cap and organic compounds impurities from the sample, respectively. The narrow contribution at −0.1 ppm can be assigned to the signal of basic hydroxyls.

The assignment of the components detected in the 3.5–5.5 ppm range, in both samples spectra, is difficult, because the chemical shift values are near those of the molecular water [15]. A comparison of NMR results with those obtained from temperature programmed desorption (TPD) experiments [16] indicates that most of the adsorbed molecular water has been desorbed by evacuating the samples at 473 K and, therefore, the components observed in Fig. 2a and b are mainly originated by hydroxyl protons. The higher intensity of the evacuated P6H spectrum compared to that of P11T indicates that P6H contains a higher hydroxyls concentration than P11T. On the other hand, though some hydroxyl bands appear in the 3.5–5.5 ppm range in both samples spectra, indicating their neutral character, the higher chemical shift value of the component at 8.3 ppm and its shoulder at 9.3 ppm indicate that part of sample P6H hydroxyls are more acidic than those of P11T, while those originating the component at −0.2 ppm are more basic. The higher hydroxylation of P6H compared to P11T indicates a higher concentration of oxygen vacancies where adsorbed water can be dissociated [17]. The strong acidity and basicity of some of the P6H hydroxyls is probably originated by the modification of the Ti–O distances in these defects, producing a different charge distribution. The hydroxyls interaction with very mobile water should hinder the hydroxyls observation in the spectra of the hydrated samples, but also originates a higher chemical shift of the water component A in the hydrated P6H spectrum, indicating the water interaction with the acidic hydroxyls. The detection of components B and C, with very low intensity, in the hydrated P6H spectrum indicates that a small amount of hydroxyls or water molecules are not affected by the anatase adsorbed water. In the case of component B, because those species were located on the rotor cap, while component C probably corresponds to species located at subsurface defects, probably, oxygen vacancies.

3.2. EPR study

Previous studies have shown that short evacuation treatments at RT, only affecting the most weakly adsorbed water, can induce significant modifications in the anatase EPR spectra [18]. In order to understand the relation between these two effects of evacuation, we have studied the influence of the anatase adsorbed water on the signals observed in the EPR spectra of P11T and P6H.

3.2.1. Photogenerated radicals in hydrated and water impregnated anatase

The spectra of hydrated P11T and P6H, UV irradiated at 77 K, were mainly originated by two anisotropic systems with orthorhombic symmetry, producing signal A, with $g_1 = 2.003$, $g_2 = 2.015$ and $g_3 = 2.025$, and signal B, with $g_1 = 2.005$, $g_2 = 2.013$ and $g_3 = 2.021$, the latter stronger for P6H than for P11T, Fig. 3a and b. Signals with g-values similar to those of signals A and B have been assigned to surface O^- ($_sO^-$) [9,19]

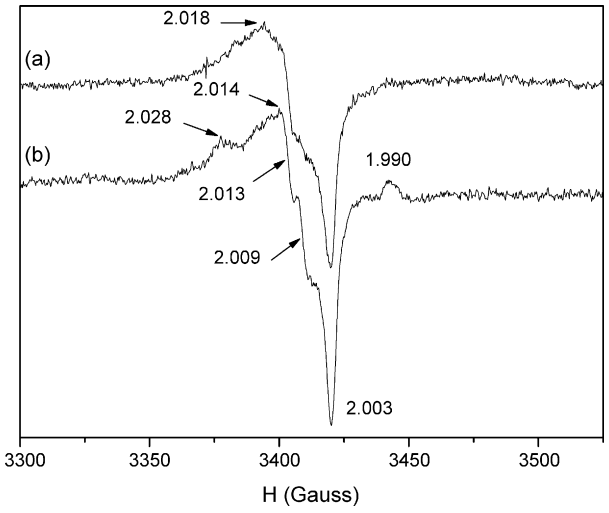

Fig. 3. EPR spectra of hydrated anatase UV irradiated at 77 K: (a) P11T and (b) P6H.

and subsurface O^- ($_bO^-$), stabilized by surface hydroxyls [19,20], respectively. The g-values and assignments of the EPR signals are collected in Table 1. The $_sO^-$ and $_bO^-$ radicals are originated by photogenerated holes trapped by low coordinate bridging O^{2-} anions [21] at surface and subsurface defects, respectively, following reactions (1) and (2).

$$_sO^{2-} + h^+ \rightarrow {}_sO^- \quad (1)$$

$$_bO^{2-} + h^+ \rightarrow {}_bO^- \quad (2)$$

As bridging O^{2-} anions are water adsorption sites [22,23], the formation of $_sO^-$ radicals should originate the desorption of water adsorbed there. The lower intensity of signal B in the P11T spectrum indicates a lower content of subsurface defects, as expected considering that this sample had been treated at higher temperature than P6H.

The P6H spectrum also showed a signal C, originated by radicals with orthorhombic symmetry with $g_1 = 2.003$, $g_2 = 2.009$ and $g_3 = 2.024$, and a peak, hereafter denoted TA, at $g = 1.990$, a g-value characteristic of the $g_\perp$ of the signal originated by Ti^{3+} cations in anatase [10,24,25], formed following reaction (3). The $g_\parallel$ component of the Ti^{3+} signal, centres with axial symmetry, is not resolved. Signals with g-values similar to those of signal C have been assigned to superoxide O_2^- radicals [26,27], formed by adsorption of molecular oxygen on photogenerated Ti^{3+} at the anatase surface, following reaction (4).

$$Ti^{4+} + e^- \rightarrow Ti^{3+} \quad (3)$$

$$Ti^{3+} + O_2 \rightarrow Ti^{4+}{-}O_2^- \quad (4)$$

The formation of O_2^- radicals indicates, therefore, that some O_2 molecules, photogenerated or not removed by evacuation at 77 K, have been adsorbed on Ti^{3+} cations, originating their oxidation and the corresponding decrease of their EPR signal.

The low intensity of the electron derived signals in relation to those originated by trapped holes in the P11T spectrum indicates that some non-recombined photogenerated electrons are not observed, either because they have originated diamagnetic species or because they were delocalized in the conduction band. The stabilization of photogenerated electrons as Ti^{3+} cations in anatase has been usually observed by EPR when working at 4.2 K [9,20] or when the concentration of defects or impurities was significant [28–30]. In the case of P6H, without impurities detectable by EPR but with very low crystal size, the observation of signal TA is favored by the presence of defects. The formation in P6H of more acidic and basic hydroxyls than in P11T, besides those observed by ^1H NMR with similar acidity in both samples spectra, indicates that these defects are oxygen vacancies, where hydroxyls are

Table 1
Assignment and g-values of the EPR signals

Signal	g_1	g_2	g_3	Assignment	Ref.
A	2.003	2.015	2.025	sO^-	[9,18]
B	2.005	2.013	2.021	$_bO^-$	[6,18,19]
C	2.003	2.009	2.024	O_2^-	[25,26]
D	2.003	2.006	2.009	O_3^-	[31,32]
E	2.003	2.009	2.034	O_2H	[33,34]
TA	$g_\perp = 1.990$, $g_\parallel = 1.960$			Ti^{3+} anatase	[10,23,24]

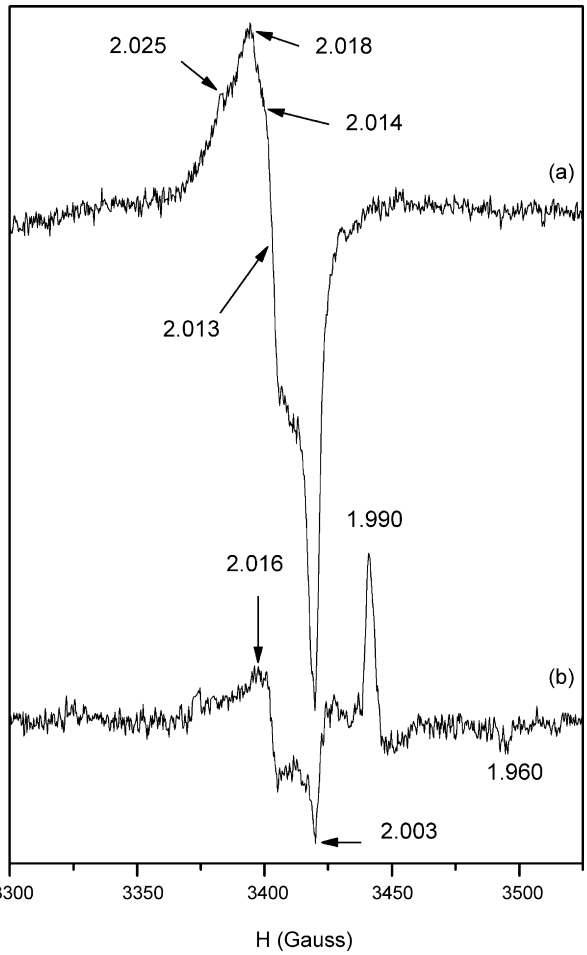

Fig. 4. EPR spectra of anatase impregnated with water and UV irradiated at 77 K: (a) P11T and (b) P6H.

formed by water dissociation [21]. Low coordinate Ti^{4+} at these vacancies are convenient trapping sites for photogenerated electrons, with the formation of Ti^{3+} cations.

The EPR spectra of the samples contacted with liquid water in the EPR cell, evacuated and UV irradiated at 77 K, were again formed mainly by signals A and B, Fig. 4a and b. The intensity of the P11T spectrum showed a significant increase, due to the increase of signal A. However, the intensity of the P6H spectrum decreased, though signal TA, with $g_{\perp} = 1.990$ and $g_{\parallel} = 1.960$, appeared with higher intensity than in the hydrated sample spectrum, Fig. 3b. These modifications indicate that the presence of frozen water at the anatase surface hinders the Ti^{3+} oxidation by adsorbed O_2, but due to this effect, the electron-hole recombination process is favored. The intensity increase of the P11T spectrum indicates that the recombination process is less effective for this sample, probably because of the easier electron delocalization in the conduction band of this less defective anatase.

3.2.2. Radicals photogenerated in anatase evacuated at 295 K

The spectra obtained after hydrated P11T and P6H were evacuated for 15 min, at RT, and irradiated at 77 K, Figs. 5a and 6a, respectively, presented lower intensity than before evacuation, Fig. 3a and b. These spectra were mainly formed by signals A and B, the latter with smaller intensity in the P11T than in the P6H spectrum, and a small signal C. The three signals were narrower in the P6H spectrum, which also shows a small Ti^{3+} signal. The decrease in the intensity of the spectra obtained after this short evacuation, which only can produce the removal of the most weakly adsorbed water [31], indicates that the removed water was favoring charge separation processes.

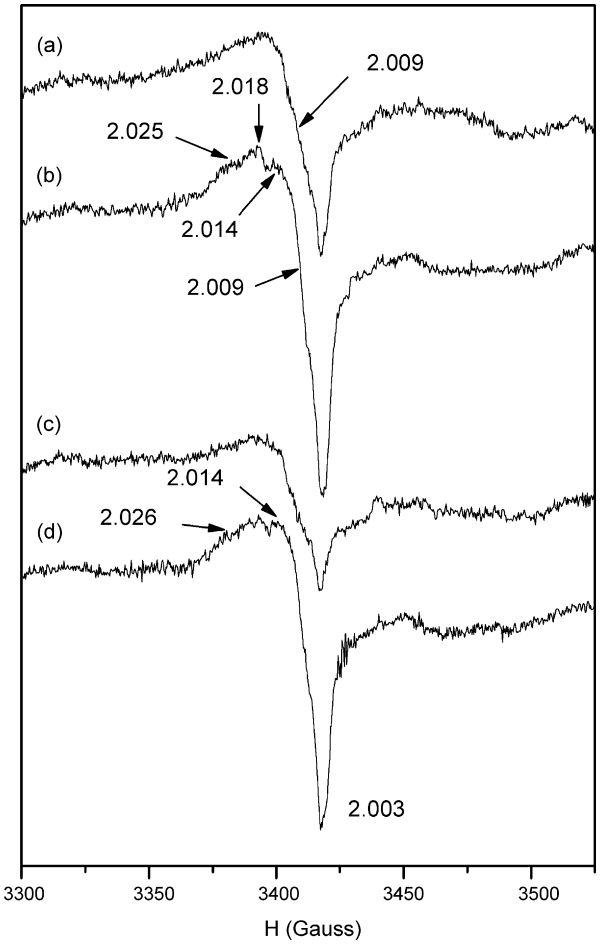

Fig. 5. EPR spectra of P11T UV irradiated at 77 K: after evacuated at 295 K for 15 min (a), subsequent O_2 adsorption at 77 K in the dark (b), after evacuation for 1 h at 295 K (c) and subsequent O_2 adsorption at 77 K in the dark (d).

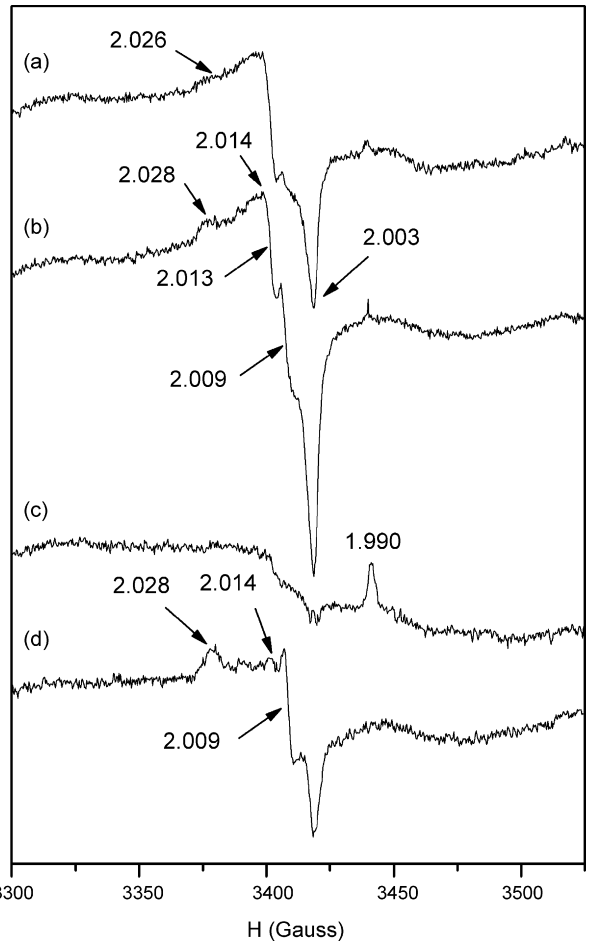

Fig. 6. EPR spectra of P6H UV irradiated at 77 K: after evacuated at 295 K for 15 min (a), subsequent O_2 adsorption at 77 K in the dark (b), after evacuation for 1 h at 295 K (c) and subsequent O_2 adsorption at 77 K in the dark (d).

A subsequent O_2 adsorption in the dark, at 77 K, on this evacuated samples produced an increase of signal C in both spectra and the disappearance of the Ti^{3+} signal from the P6H spectrum, Figs. 5b and 6b. The formation of O_2^- radicals indicates that adsorbed O_2 had trapped photogenerated electrons from both samples. These electrons were at least partially captured from Ti^{3+} cations of P6H, but in the case of P11T, these trapped electrons should have been delocalized in the conduction band.

The spectra obtained after fresh hydrated P11T and P6H samples were evacuated at RT for 1 h and irradiated at 77 K were mainly formed by signals A and B, with signal TA also contributing to the P6H spectrum, Figs. 5c and 6c. The intensity of the spectra was lower than that of the spectra obtained after

the short samples outgassing and irradiation, being the decrease particularly marked in the P6H spectrum. The progressive decrease of signals A and B with evacuation time confirms that the weakly adsorbed water is favoring the stabilization of photogenerated holes as O^- species. A subsequent contact of this partially dehydrated and irradiated samples with oxygen at 77 K, in the dark, produced again a marked increase of signal C and the disappearance of signal TA from the P6H spectrum, Figs. 5d and 6d. The more marked increase of signal C for P11T than for P6H indicates that the trapping of delocalized electrons by adsorbed O_2 is easier in P11T, due to its lower defects content.

Though photogenerated holes can be stabilized as O^- radicals at low coordinate bridging O^{2-} anions, these anions can also form bridging hydroxyls, particularly in anatase samples with a significant concentration of oxygen vacancies, by inducing water dissociation. The more marked influence of the weakly adsorbed water on signal A intensity in the EPR spectra of P6H, the anatase presenting the most acidic hydroxyls, seems to indicate that, when O^- radicals are formed by photogenerated holes stabilization at the acidic hydroxyls O^{2-} anions, water interacting with these hydroxyls can be desorbed together with the hydroxyls protons, as H_3O^+ species. The proton exchange between H_3O^+ species and adsorbed water can facilitate the H_3O^+ desorption and O^- formation. On the other hand, the removal of adsorbed water should hamper the protons exchange process, stabilizing the water interacting with acidic hydroxyls and hindering the holes localization at the low coordinate bridging O^{2-} anions of these hydroxyls.

3.2.3. Radicals photogenerated in anatase in the presence of adsorbed oxygen.

The spectra obtained for P11T and P6H evacuated at RT and irradiated at 77 K, in the presence of adsorbed O_2, are mainly formed by signals A, B and C, Fig. 7a and b. Small shoulders at $g = 2.009$ and 2.034 in the P11T and P6H spectra, respectively, indicate the formation of O_3^- [32,33], and O_2H species [34,35]. These radicals, with orthorhombic symmetry, originate signals

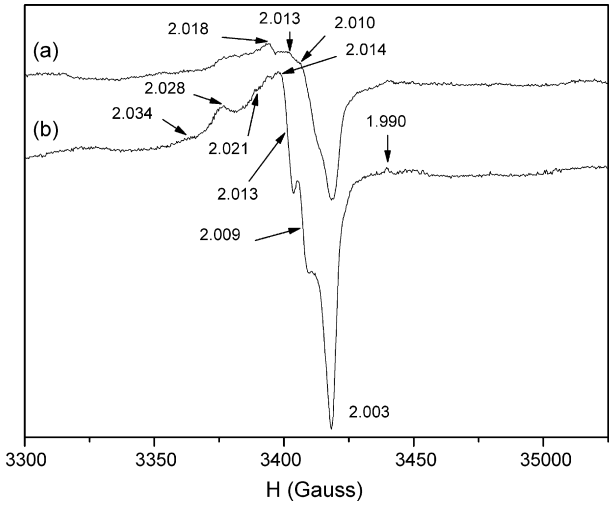

Fig. 7. EPR spectra of anatase evacuated for 1 h and UV irradiated at 77 K in the presence of adsorbed O_2: (a) P11T and (b) P6H.

with $g_1 = 2.003$, $g_2 = 2.006$ and $g_3 = 2.009$, signal D, and with $g_1 = 2.003$, $g_2 = 2.009$ and $g_3 = 2.034$, signal E. The photogenerated holes derived species O_3^- is formed by O_2 interaction with surface O^- radicals and the electron derived O_2H are produced by O_2^- protonation, following reactions (5) and (6), respectively.

$$_sO^- + O_2 \rightarrow {}_sO_3^- \quad (5)$$

$$O_2^- + H^+ \rightarrow O_2H \quad (6)$$

The higher intensity of the P6H spectrum is probably due to the generation of Ti^{3+} cations at oxygen vacancies. The presence of these cations facilitates the electron trapping by adsorbed O_2, generating O_2^- and O_2H species, inducing the stabilization as O^- and O_3^- radicals of non-recombined holes. The low concentration of defects in P11T hampers the formation of Ti^{3+} cations, but favors the delocalization of photogenerated electrons in the conduction band. The presence of these electrons facilitates the generation of Ti^{4+}–O_2^- species, but also induces the stabilization of $_sO_3^-$ radicals formed by O_2 adsorption on $_sO^-$ sites.

4. Conclusions

The EPR and ^1H NMR spectra show that the characteristics of the water and hydroxyls adsorbed on thermally and hydrothermally treated anatase, and the type of radicals photogenerated in these samples, present some significant differences. Both hydrated samples retain highly mobile adsorbed water, more abundant in P6H than in P11T. P6H also retains a larger amount of hydroxyls than P11T, some of them with chemical shifts markedly different from those observed in P11T spectra. The presence of similar amounts of acidic and basic hydroxyls on P6H indicates that they are formed by water dissociation at oxygen vacancies. The EPR spectra at 77 K of the samples impregnated with an excess of water show the formation of surface and subsurface O^- radicals, originated by hole stabilization at surface bridging O^{2-} anions and at subsurface defects, but also of Ti^{3+} cations in P6H. The detection of these cations at 77 K in P6H, but not in P11T, indicates that they are formed at defects, probably oxygen vacancies. The intensity of the photogenerated holes derived signals, observed in the hydrated samples spectra, decreased by increasing the evacuation time at 295 K, more markedly for P6H than for P11T. This modification indicates that the most weakly adsorbed water contributes to the photogenerated holes stabilization at low coordinate bridging O^{2-} anions, by helping the desorption of adsorbed water and hydroxyls protons from acidic hydroxyls as H_3O^+ species, keeping the protons delocalized in the water layer.

The type of radicals formed by UV irradiation in the presence of adsorbed oxygen depends on the photogeneration of Ti^{3+} cations. Thus, O_2^- radicals are mainly formed on P6H because, due to its high concentration of surface oxygen vacancies, Ti^{3+} cations are easily formed. On the other hand, the incorporation of photogenerated electrons to the conduction band facilitates the formation of O_3^- radicals on P11T.

Acknowledgements

This study has received financial support from the projects MAT2001-2112-C01-01 and CTQ2004-034097/BQU, funded by the Spanish *Ministerio de Educación y Ciencia* (MEC). FF and MDHA want to thank MEC and the *Comunidad de Madrid*, respectively, for the award of their doctoral grants.

References

[1] N. Serpone, E. Pelezzetti, Photocatalysis Fundamentals and Applications, Wiley-Interscience, New York, 1989.
[2] Heterogeneous Photocatalysis, M. Schiavello (Ed.), Wiley Series in Photoscience and Photoengineering, vol. 3, J. Wiley & Sons, Chichester, 1997.
[3] M.A. Henderson, W.S. Epling, C.H.F. Peden, C.L. Perkins, J. Phys. Chem. B 107 (2003) 534.
[4] I. Bedja, P.V. Kamat, J. Phys. Chem. 99 (1995) 9182.
[5] M.R. Hoffmann, S.T. Martin, W. Choi, D.W. Bahnemann, Chem. Rev. 95 (1995) 69.
[6] V. Stone, K. Donaldson, Nature Nanotech. 1 (2006) 23.
[7] G. Martra, V. Augugliaro, S. Coluccia, E. García-López, V. Loddo, L. Marchese, L. Palmisano, M. Schiavello, Stud. Surf. Sci. Catal. 130 (2000) 665.
[8] K.L. Yeung, A.J. Maira, J. Stolz, E. Hung, N. Ka-Chung Ho, A.C. Wei, J. Soria, K.J. Chao, P.L. Yue, J. Phys. Chem. B 106 (2002) 4608.
[9] R.F. Howe, M. Grätzel, J. Phys. Chem. 91 (1987) 3906.
[10] R.F. Howe, M. Grätzel, J. Phys. Chem. 89 (1985) 1498.
[11] A.J. Maira, K.L. Yeung, J. Soria, J.M. Coronado, C. Belver, C.Y. Lee, V. Augugliario, Appl. Catal. B 29 (2001) 327.
[12] A.J. Maira, J.M. Coronado, V. Augugliaro, K.L. Yeung, J.C. Conesa, J. Soria, J. Catal. 202 (2001) 413.
[13] A.J. Maira, K.L. Yeung, C.Y. Lee, P.L. Yue, C.K. Chan, J. Catal. 192 (2000) 185.
[14] A.Y. Nosaka, T. Fujiwara, H. Yagi, H. Akutsu, Y. Nosaka, J. Phys. Chem. B 108 (2004) 9121.
[15] A.Y. Nosaka, Y. Nosaka, Bull. Chem. Soc. Jpn. 78 (2005) 1595.
[16] M. Egashira, S. Kawasumi, S. Kagawa, T. Seiyama, Bull. Chem. Soc. Jpn. 51 (1978) 3144.
[17] M.A. Henderson, Surf. Sci. Rep. 46 (2002) 1.
[18] J.M. Coronado, A.J. Maira, J.C. Conesa, J. Soria, NATO Sci. Ser. II, Math. Phys. Chem. 76 (2002) 297.
[19] Y. Nakaoka, Y. Nosaka, J. Photochem. Photobiol. A: Chem. 110 (1997) 299.
[20] O.I. Micic, Y. Zhang, K.R. Cromack, A.D. Trifunac, M.C. Thurnauer, J. Phys. Chem. 97 (1993) 7277.
[21] M.A. Henderson, Langmuir 12 (1996) 5098.
[22] G.S. Herman, Z. Dohnálek, N. Ruzycki, U. Diebold, J. Phys. Chem. 107 (2003) 2788.
[23] A. Tilocca, A. Selloni, J. Phys. Chem. B 108 (2004) 4743.
[24] M. Che, P.C. Gravelle, P. Meriaudeau, C.R. Acad. Sci. Paris 2868C (1969) 768.
[25] J.C. Conesa, M.T. Sainz, J. Soria, G. Munuera, V. Rives-Arnau, A. Muñoz, J. Mol. Catal. 17 (1982) 231.
[26] P. Meriaudeau, M. Che, P.C. Gravelle, S. Teichner, Bull. Soc. Chim. Fr. 1 (1971) 12.
[27] C. Naccache, P. Meriaudeau, M. Che, A.J. Tench, J. Chem. Soc. Faraday Trans. 67 (1971) 506.
[28] J. Kiwi, J.T. Suss, S. Szopiro, Chem. Phys. Lett. 106 (1984) 135.
[29] M. Okumura, J.M. Coronado, J. Soria, M. Haruta, J.C. Conesa, J. Catal. 203 (2001) 168.
[30] J.M. Coronado, A.J. Maira, A. Martínez-Arias, J.C. Conesa, J. Soria, J. Photochem. Photobiol. A: Chem. 150 (2002) 213.
[31] D.D. Beck, J.M. White, C.T. Ratcliffe, J. Phys. Chem. 90 (1986) 3123.
[32] P. Meriaudeau, J.C. Vedrine, J. Chem. Soc. Faraday I 72 (1976) 472.
[33] A.R. González-Elipe, G. Munuera, J. Soria, J. Chem. Soc. Faraday Trans. I 75 (1979) 748.
[34] D.C. McCain, W.E. Palke, J. Magn. Reson. 20 (1975) 52.
[35] J.M. Coronado, A.J. Maira, J.C. Conesa, K.L. Yeung, V. Augugliaro, J. Soria, Langmuir 17 (2001) 5368.